



ELSEVIER

Physica A 240 (1997) 286–296

83184

PHYSICA A

Simulation of two-dimensional Kolmogorov flow with smooth particle applied mechanics

H.A. Posch^{a,*}, W.G. Hoover^b

^a *Institut für Experimentalphysik, Universität Wien, Boltzmannngasse 5, A-1090 Wien, Austria*

^b *Department of Physics, Lawrence Livermore National Laboratory and Department of Applied Science, University of California at Davis/Livermore, Livermore, CA 94551-7808, USA*

Abstract

Smooth-particle applied mechanics is an interesting alternative method for the simulation of hydrodynamic flows. In this grid-free procedure the various fields are calculated by summing up the contributions from neighboring particles which are smoothly distributed in space according to a weighting function. The motion equations for these particles are ordinary differential equations similar – and in special cases isomorphic – to the atomistic equations of motion. We apply the method to two-dimensional Kolmogorov flow, where the fluid in the top and bottom half of the tube is accelerated in opposite directions. By varying the Reynolds number the transition from laminar flow to a stationary flow with symmetrically placed vortices is followed.

PACS: 02.70.-c; 02.70.Ns; 47.11.+j; 47.15.-x; 47.20.-k

1. Introduction

Computer simulations of compressible hydrodynamic flows are usually carried out with finite-difference and finite-element methods [1] using either fixed (Eulerian) or co-moving (Lagrangian) grids. Alternatively, particle methods have been developed [2] which do not suffer from the instabilities inherent to grid-based techniques [3]. Almost simultaneously and independently, Lucy [4], and Gingold and Monaghan [5] developed a scheme by combining the concept of particles with that of a smoothing or weight function $w(r; h)$ of finite range h , with which any field variable $f(r)$ at location r may be interpolated from its values $f_j \equiv f(r_j)$ at the positions r_j of the SPAM particles by

$$f(r) = \sum_j \frac{m_j}{\rho_j} f_j w(|r - r_j|; h), \quad (1)$$

* Corresponding author. Tel.: +43-1-31367 3109; fax: +43-1-3102683; e-mail: posch@ls.exp.univie.ac.at

where m_j and ρ_j are the mass and the mass density associated with the j th particle. Their method, known as “smoothed particle hydrodynamics” was subsequently applied mainly to astrophysical problems [6–9], until its usefulness for problems in conventional solid and fluid mechanics was recognized [10–14]. We therefore refer to this method as smooth-particle applied mechanics (SPAM). It was successfully applied to viscous Couette flows [12,13], to Poiseuille flow and flow around cylinders [11], and to a study of the onset of Rayleigh–Bénard convection [13].

The conservation equations of continuum mechanics in the Lagrangian, comoving-derivative formulation are given by

$$\dot{\rho} = -\rho \nabla \cdot \mathbf{v}, \quad (2)$$

$$\rho \dot{\mathbf{v}} = \nabla \cdot \boldsymbol{\sigma} + \rho \mathbf{g}, \quad (3)$$

$$\rho \dot{e} = \nabla \mathbf{v} : \boldsymbol{\sigma} - \nabla \cdot \mathbf{q}, \quad (4)$$

where ρ is the mass density, \mathbf{v} the flow velocity, $\boldsymbol{\sigma}$ the stress tensor, e the energy per unit mass, and \mathbf{q} the heat flux vector. An external body force is accounted for by an acceleration \mathbf{g} . In the particle representation of SPAM these partial differential equations are transformed into a set of ordinary differential equations for the position \mathbf{r}_i , and the field quantities \mathbf{v}_i and e_i associated with particles i . The formulation of the motion equations depends upon the choice of representation for the field gradients, and is far from unique. The following set of equations was shown to yield good results for conventional fluid flows, where the equations are arranged in the same sequence as they would appear in an actual program:

(a) Computation of the mass densities ρ_i for the particles i :

$$\rho_i = \sum_j m_j w_{ij}. \quad (5)$$

(b) Computation of the velocity-derivative tensor $(\nabla \mathbf{v})_i$ and temperature gradient $(\nabla T)_i$ associated with particle i :

$$(\nabla \mathbf{v})_i = \sum_j \frac{m_j}{\rho_{ij}} [\mathbf{v}_j - \mathbf{v}_i] \nabla_i w_{ij}, \quad (6)$$

$$(\nabla T)_i = \sum_j \frac{m_j}{\rho_{ij}} [T_j - T_i] \nabla_i w_{ij}, \quad (7)$$

where ρ_{ij} is a mean density for the particle pair i, j , usually the geometric mean. This particular representation for the gradients of flux-generating variables has even parity with respect to interchange of particles i and j provided $m_i = m_j$.

For the flows of conserved variables, such as the momentum and energy fluxes, a useful representation of the space derivatives of the stress tensor $\boldsymbol{\sigma}$ and heat flux vector \mathbf{q} requires odd parity with respect to particle interchange ($m_i = m_j$) to assure

the conservation of energy and linear momentum:

$$\frac{(\nabla \cdot \boldsymbol{\sigma})_i}{\rho_i} = \sum_j m_j \left[\frac{\boldsymbol{\sigma}_i}{\rho_i^2} + \frac{\boldsymbol{\sigma}_j}{\rho_j^2} \right] \cdot \nabla_i w_{ij}, \quad (8)$$

$$\frac{(\nabla \cdot \mathbf{q})_i}{\rho_i} = \sum_j m_j \left[\frac{\mathbf{q}_i}{\rho_i^2} + \frac{\mathbf{q}_j}{\rho_j^2} \right] \cdot \nabla_i w_{ij}. \quad (9)$$

(c) Mechanical and thermal equations of state $p(\rho, e)$ and $T(\rho, e)$, respectively, for the computation of the pressure p_i and temperature T_i associated with i . At this stage the properties of the fluid enter.

(d) Newtonian and Fourier constitutive relations for the transport of momentum and energy, specifying the stress tensor $\boldsymbol{\sigma}_i$ and heat-flux vector \mathbf{q}_i associated with particle i :

$$\boldsymbol{\sigma}_i = -p_i \mathbf{I} + \eta \left\{ (\nabla \mathbf{v})_i + (\nabla \mathbf{v})_i^T - \frac{2}{d} (\nabla \cdot \mathbf{v})_i \mathbf{I} \right\} + \eta_V (\nabla \cdot \mathbf{v})_i \mathbf{I}, \quad (10)$$

$$\mathbf{q}_i = -\kappa (\nabla T)_i. \quad (11)$$

Here, η is the shear viscosity, η_V the volume or “bulk” viscosity, and κ is the heat conductivity. d denotes the dimension of space, two or three, \mathbf{I} is a unit tensor, and the superscript T denotes transposition.

(e) Finally, a useful set of equations of motion for the SPAM particles are

$$\dot{\mathbf{r}}_i = \mathbf{v}_i, \quad (12)$$

$$\dot{\mathbf{v}}_i = \sum_j m_j \left[\frac{\boldsymbol{\sigma}_i}{\rho_i^2} + \frac{\boldsymbol{\sigma}_j}{\rho_j^2} \right] \cdot \nabla_i w_{ij} + \mathbf{g}_i, \quad (13)$$

$$\dot{e}_i = \sum_j \frac{m_j}{2} \left[\frac{\boldsymbol{\sigma}_i}{\rho_i^2} + \frac{\boldsymbol{\sigma}_j}{\rho_j^2} \right] : (\mathbf{v}_j - \mathbf{v}_i) \nabla_i w_{ij} - \sum_j m_j \left[\frac{\mathbf{q}_i}{\rho_i^2} + \frac{\mathbf{q}_j}{\rho_j^2} \right] \cdot \nabla_i w_{ij}. \quad (14)$$

In all these equations $w_{ij} \equiv w(|\mathbf{r}_i - \mathbf{r}_j|; h)$, and $\nabla_i w_{ij}$ means that the gradient is to be evaluated at the position of particle i . The particular representation for the space derivatives in Eqs. (6)–(9) with the indicated symmetry with respect to particle interchange assures that motion equations (13) and (14) conserve linear momentum and energy exactly for bulk flow. We want to stress that these equations are by no means unique [7,11], although they have already been shown to give good results for a variety of simple bulk flows.

The choice of the weighting function w strongly affects the actual appearance of the evolving pattern of particles but not that of the SPAM-averaged fields computed from Eq. (1) [13,15]. In this work a function introduced by Lucy [4] is used,

$$w(r; h) = \begin{cases} c_w (1 + 3q)(1 - q)^3 & \text{for } r \leq h, \\ 0 & \text{for } r > h, \end{cases} \quad (15)$$

where $q = r/h$, has continuous first and second derivatives at the cutoff distance h and has been shown to give flow fields conforming to theoretical expectations in the case of Rayleigh–Bénard convection. In (15) the normalization constant becomes $c_w = 5/(\pi h^2)$ in two dimensions, and $c_w = 105/(16\pi h^3)$ in three. This function is used in this paper for all our numerical work, with $h = 3$ in proper reduced units. A corresponding-states principle has been shown to exist if all distances are scaled according to h [14]. It is worth mentioning that in two dimensions about 20–30 other particles should be within the interaction range h of a particle to obtain a faithful representation of the flow [15]. In three dimensions this number goes up to about 80. It follows that the total number of particles for a typical SPAM simulation will usually be large, calling for time-saving techniques such as linked lists.

In the next section we apply SPAM, formally represented by Eqs. (5)–(15), to the special case of an ideal gas with an equation of state $p = C\rho^2$, where C is a constant – ultimately set to unity in our reduced units – and vanishing transport coefficients η, η_V , and κ . We have shown already in Ref. [12] that such a fluid – in spite of $\eta = 0$ – possesses an intrinsic shear viscosity η_0 , which is a consequence of the finite number of particles representing the fluid flow, and which vanishes in the limit of $N \rightarrow \infty$. Similarly, such a fluid also exhibits an intrinsic heat conductivity [16]. We also present simulations of Kolmogorov flow for a very similar fluid and demonstrate the transition from laminar flow to other states characterized by stationary vortices.

2. Planar Kolmogorov flow for an ideal gas

For the special case of an isentropic ideal gas with $p_i = C\rho_i^2$, and vanishing η, η_V , and κ , the equations of motion (13) simplify considerably and become isomorphic to those of molecular dynamics with $2Cm^2w(r; h)$ playing the role of a pair potential [15]. The energy equation (14) is no longer required for the computation of the trajectory and, in fact, becomes identical to the usual equation for conservation of energy in molecular dynamics. Like any other particle system, such a SPAM fluid exhibits an intrinsic shear viscosity η_0 and heat conductivity κ_0 which describe the macroscopic flow of momentum and energy in the smooth-particle representation of the corresponding continuum flow in spite of a possible vanishing η, η_V , and κ . They are artifacts of the finite number of particles representing the flow and correspond to the kinetic contributions to the shear viscosity and heat conductivity of an equivalent atomic system. These intrinsic transport properties impose upper bounds on the Reynolds and Rayleigh numbers of the flows accessible to SPAM. Since the intrinsic transport coefficients, viscosity and heat conductivity, seem to vary with the particle number at least as strong as N^{-2} , higher Reynolds and Rayleigh numbers are more easily accessible by SPAM.

We have recently determined the intrinsic shear viscosity for such a two-dimensional fluid [12] with a homogeneous nonequilibrium molecular dynamics technique. We take

N particles in a box and use reduced units for which the reduced box volume is given by $V = L_x L_y$ and the range of the weighting function is $h = 3$. The reduced mass m , taken to be equal for all the particles, is determined from the requirement that the total mass per unit volume be unity, $Nm/V = 1$. This assures that the SPAM density ρ_i of a particle is also close to unity in our reduced units. Furthermore, the unit of energy is $2Cm^2(9\pi/5)w(r=0; h=3)$, and a temperature scale is used for which Boltzmann's constant k is unity. In the low-density limit the dependence of η_0 on the temperature and the interaction length h of the Lucy "pair potential" may be expressed in these units as [14]

$$\eta_0(T; h) = [0.24(mkT)^{1/2}/h][1 + 4(kTh^2)^2]. \quad (16)$$

We have estimated the heat conductivity for two different temperatures, 0.07 and 0.54, employing an inhomogeneous nonequilibrium molecular dynamics method with two thermostatted boxes, one cold and one hot, separated by unthermostatted regions for which the heat flux is determined [16]. We find that the fictitious heat conductivity is of the same order of magnitude as η_0 , in rough agreement with kinetic theory predicting $\kappa_0 = 4\eta_0$ in our reduced units.

To check the hydrodynamic behavior of such a SPAM fluid we report here simulations of two-dimensional channel flow parallel to the x -axis. We were particularly interested in the transition from laminar to turbulent flow. To avoid the complication introduced by no-slip boundary conditions we consider in this section so-called Kolmogorov flow along the x -direction. This flow is driven by a body force causing an acceleration $\mathbf{g} = g(y)\hat{\mathbf{x}}$ parallel to x and periodic in the transverse direction [17–19] with period $2\pi/k_y$. It is characterized by parallel channels of width $L_y/2 = \pi/k_y$ and alternating flow directions. Assuming the fluid to be incompressible, the laminar velocity profile is readily obtained from (13). If the body force varies sinusoidally in the transverse y -direction, as indicated in Fig. 1, $g(y) = g_0 \sin(k_y y)$, the steady-state solution of (3) becomes

$$\mathbf{v} = v_0 \sin(k_y y) \hat{\mathbf{x}}, \quad (17)$$

where

$$v_0 = \frac{g_0}{\nu k_y^2}, \quad (18)$$

and $\nu = \eta/\rho$ is the kinematic viscosity. In this paper, $\hat{\mathbf{x}}$ and $\hat{\mathbf{y}}$ denote unit vectors in the indicated directions.

The Kolmogorov flow is known to be unstable to long-wave-length fluctuations. If the Reynolds number, given for equilibrium flow by $R = g_0/(\nu^2 k_y^3)$ exceeds a critical value $R_0 = \sqrt{2}$, a secondary steady flow develops showing stationary eddies arranged in a regular pattern [18,19]. This critical threshold R_0 applies only to the limiting case of infinitely long channels permitting fluctuations with very large wave lengths. For a non-vanishing aspect ratio $\alpha = L_y/L_x$ the critical Reynolds number increases significantly

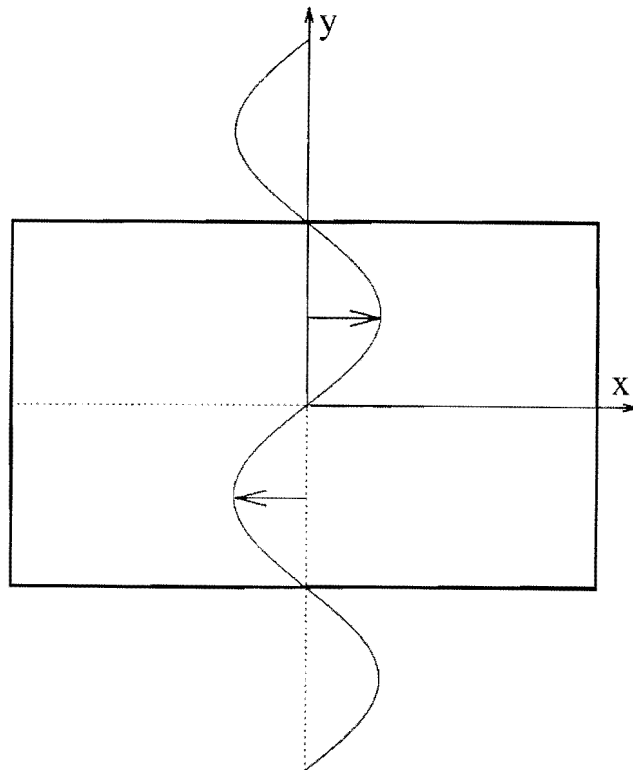


Fig. 1. Kolmogorov flow for a sinusoidally varying force with wave vector k_y and a sinusoidal velocity profile. The simulation box with length L_x and width $L_y = 2\pi/k_y$ is also shown. Periodic boundary conditions both in x - and y -direction are applied.

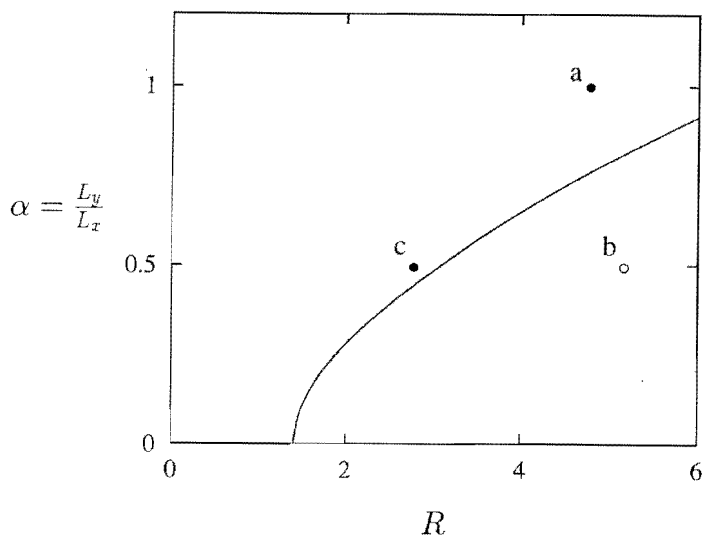


Fig. 2. Qualitative shape of the line of marginal stability for laminar flow (solid line), where R is the Reynolds number, and L_y/L_x is the aspect ratio. The labeled points refer to the respective flows depicted in Fig. 3 and are discussed in the text.

[17–19]. The marginal line of stability is shown qualitatively in Fig. 2 and is not truly to scale. The secondary state with stationary eddies is itself unstable and periodic oscillations develop for Reynolds numbers $R \approx 2.5R_0$ [19]. For even higher R a cascade

of ever smaller eddies and higher harmonics become significant until a turbulent state is reached.

A reformulation of the continuum Eqs. (2)–(4) in SPAM language is provided by Eqs. (5)–(14), with one modification: The kinetic energy of the flow continuously generated by the body force is converted into heat and through heat conduction and internal friction raises the total internal energy

$$\int \rho(\mathbf{r})e(\mathbf{r}) d\mathbf{r} = \sum_i m_i e_i. \quad (19)$$

To achieve a steady flow, this heat rate must be counteracted by an energy sink in the energy-rate equation (14). This is achieved by adding a constraining term $-\zeta e_i$ to the right-hand side of (14). The Lagrange parameter ζ is determined from the condition that the energy (19) be exactly constrained:

$$\zeta = \frac{\sum_i m_i \dot{e}_i}{\sum_i m_i e_i}. \quad (20)$$

For our Kolmogorov flow simulations we use the ideal-gas equation of state

$$p = \rho e = \rho kT/m. \quad (21)$$

We take equal masses m for all particles and use the same reduced units as before. The simulation box with length L_x and width $L_y = 2\pi/k_y$ is shown in Fig. 1. Periodic boundary conditions are applied both parallel and transverse to the flow. Number densities of 1 and 4 corresponding to respective particle masses of 1 and 0.25 are used, and, as before, $h=3$ is chosen for the range of Lucy's weight function. Since the theoretical analysis mentioned above was carried out for an incompressible fluid, we approach this condition by choosing a rather large heat conductivity $\kappa=5$ in our reduced units. This prevents very effectively large variations of e_i , ρ_i , and p_i and makes the density uniform aside from small fluctuations inherent to the SPAM method. Alternatively, the incompressible limit could be achieved by using a high internal energy. The SPAM density according to (5) is always close to 1 in our simulation. The shear and bulk viscosities are chosen to vanish, $\eta = \eta_V = 0$, and the frictional momentum transport is solely due to the intrinsic viscosity η_0 mentioned above.

We consider the following examples:

(A) In Fig. 3(a) the flow of 1600 particles in a box with $L_x = L_y = 40$, aspect ratio $\alpha \equiv L_y/L_x = 1$, and mass $m = 1$ is shown. The acceleration g_0 is 0.01. The time-averaged velocity profile $\langle v_x(y) \rangle$ is sinusoidal and is depicted in Fig. 4(a) by the full line. The little bars attached to the particles are proportional to their SPAM-smoothed velocities computed with Eq. (1). Instantaneous velocity profiles are indicated by broken lines in Fig. 4. There are spontaneous short-wave-length fluctuations present in this flow, but they are short lived and do not increase. The flow is stable, and from the amplitude of the sinusoidal velocity profile, $v_0 = 0.55$, and Eq. (18) we obtain $v = 0.74$ corresponding to a Reynolds number $R = 4.8$. In the phase plot of Fig. 2 the respective point is labelled "a".

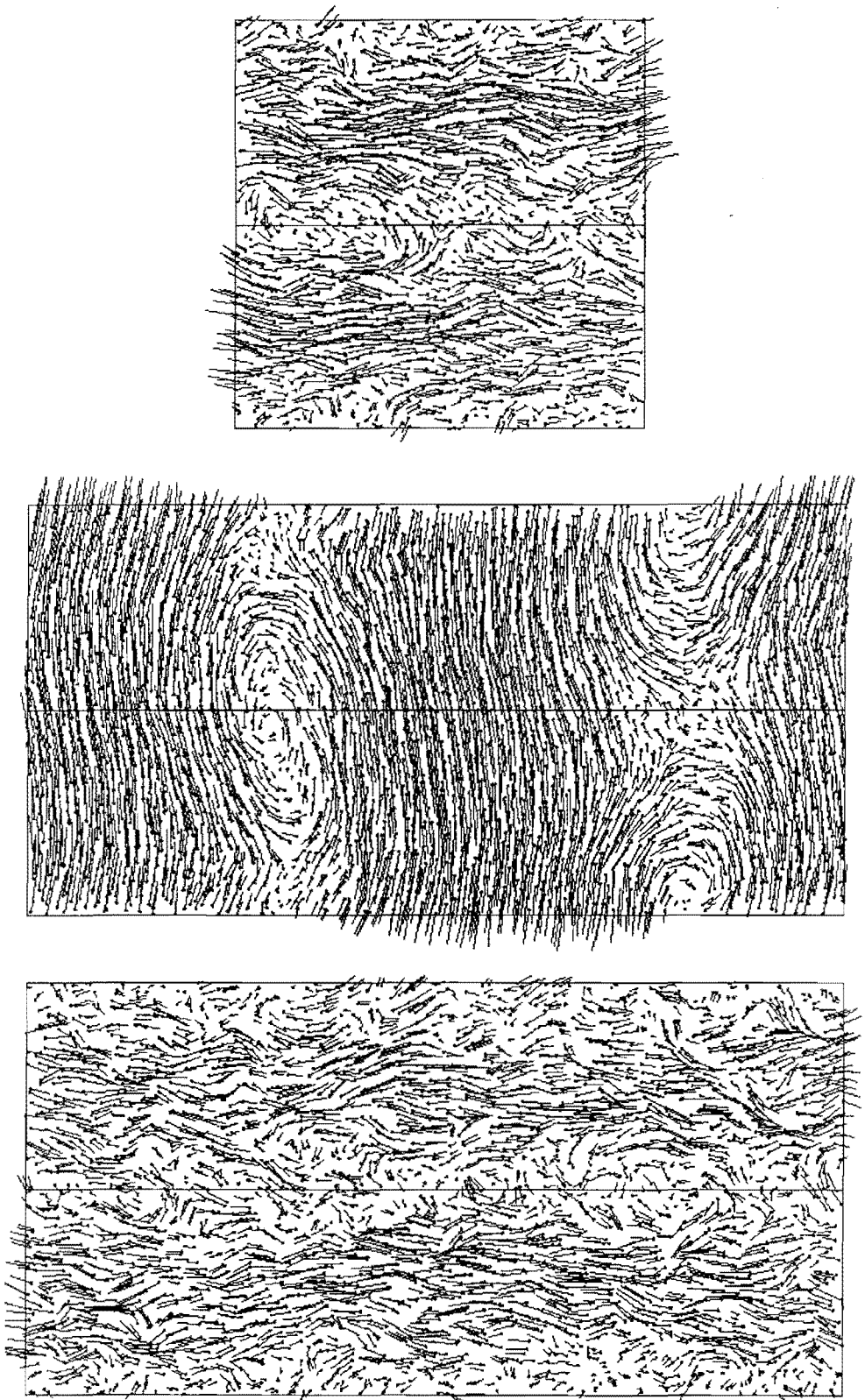


Fig. 3. Kolmogorov flows as discussed in the text: (a) (top) 1600 particles of mass 1 in a box ($L_x = 40$, $L_y = 40$, aspect ratio 1) with periodic boundaries. The driving amplitude $g_0 = 0.01$. (b) (middle) 3200 particles of mass 1 in a box ($L_x = 80$, $L_y = 40$, aspect ratio 0.5) with periodic boundaries. The driving amplitude $g_0 = 0.01$. (c) (bottom) 3200 particles of mass 1 in a box ($L_x = 80$, $L_y = 40$, aspect ratio 0.5) with periodic boundaries. The driving amplitude $g_0 = 0.02$.

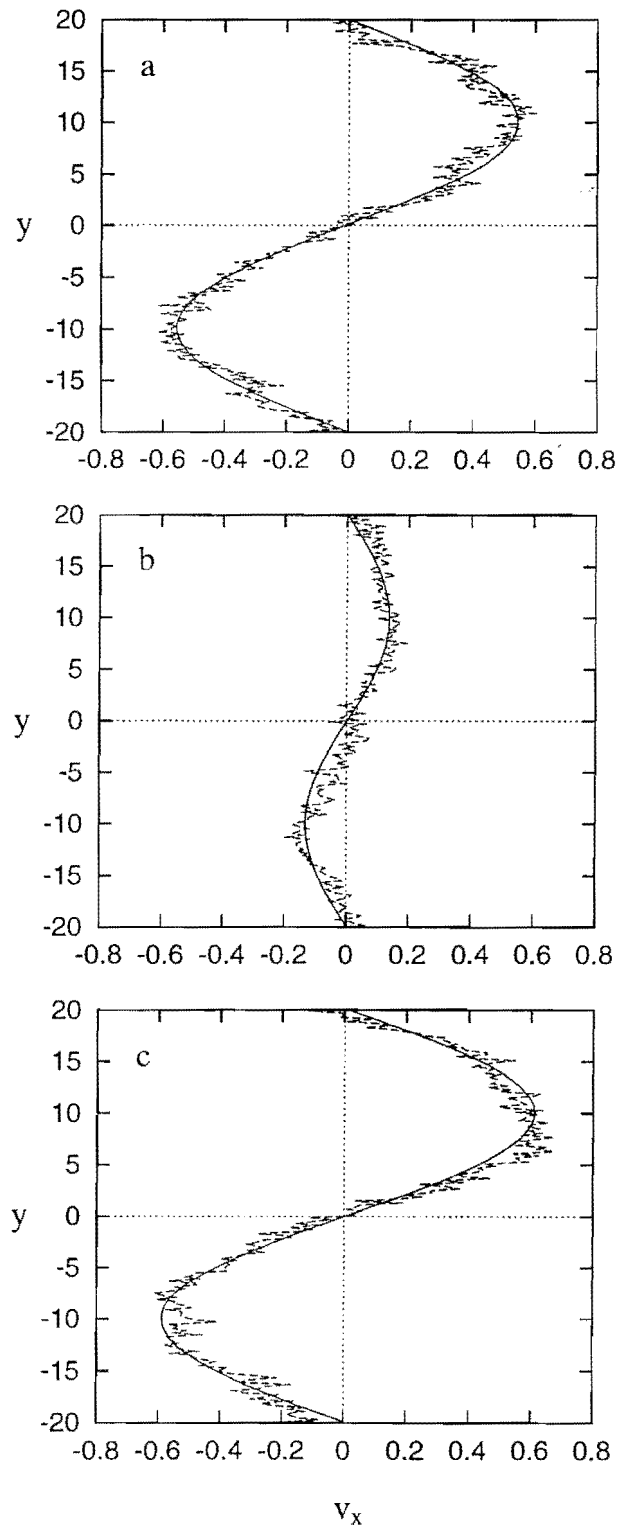


Fig. 4. Velocity profiles for the flows in Fig. 3. The full curves are time averaged profiles, the dashed curves are instantaneous SPAM velocity profiles, where the SPAM velocity of a particle was computed with the help of Eq. (1). The labels a to c correspond to those in Fig. 3.

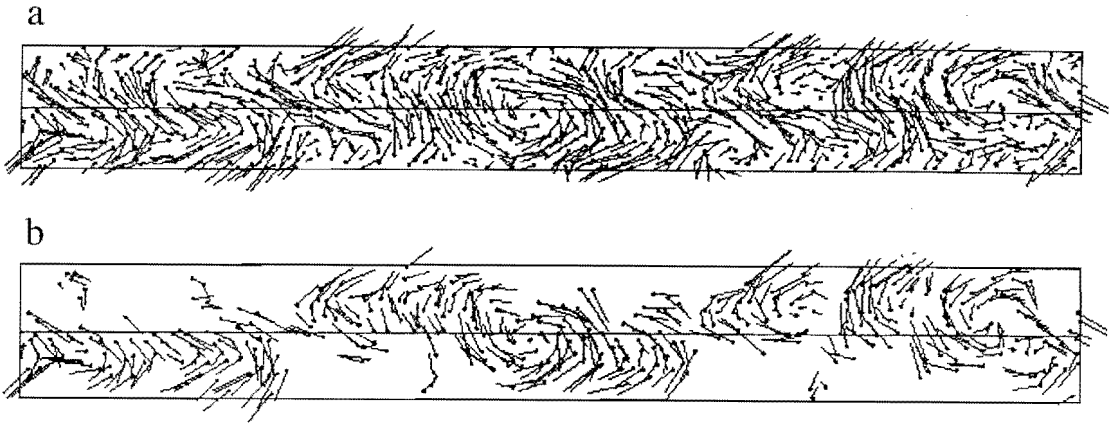


Fig. 5. Turbulent flow for a system of 800 particles of mass 1 in a box of size 80×10 . The driving field amplitude g_0 is 0.005. In (a) all particles are shown, in (b) only those with a negative vorticity.

(B) If we increase L_x to 80 and double also the number of particles, leaving all other parameters unchanged, the stationary flow depicted in Fig. 3(b) is obtained. This flow is characterized by two stationary symmetrically placed vortices, and its location in the phase plot is qualitatively marked by a point labelled “b”. The velocity profile in Fig. 3(b) is still sinusoidal, although with a vastly reduced amplitude. Since Eq. (18) does not apply any more, there is at present no reliable way of computing the viscosity and the Reynolds number for this flow.

(C) In the next example all parameters are as in case B with the exception of the field amplitude g_0 which is *increased* to 0.02. The – at first glance paradoxical – flow pattern is shown in Fig. 3(c), the respective velocity profile in Fig. 4(c). In spite of an increase of g_0 a regular flow with a Reynolds number $R=2.8$ is obtained. The reason for this unusual behavior lies in the local kinetic temperature increase in our ideal-gas SPAM fluid which in turn leads to an increase [12] of the intrinsic kinematic viscosity to $\nu=1.35$, larger than in example (A). The state point for this flow lies in the stable region to the left of the marginal stability curve in Fig. 2 and is labelled “c”.

From these examples one concludes that SPAM qualitatively reproduces the transition from a laminar to a secondary stationary flow characterized by an array of stationary vortices. If the Reynolds number is further increased, this secondary flow becomes unstable again. In Fig. 5 such a case is depicted for a system of 800 particles of mass 1 in a box of size 80×10 . The driving field amplitude g_0 is 0.005. In Fig. 5(a) all particles are shown, in Fig. 5(b) only those with a negative vorticity. Thus, also the transition to fully developed turbulence is accessible by this method. The unsolved problem we face is the determination of the Reynolds number in the unstable regime. One not yet exploited possibility seems to be the determination of the local kinetic temperature from the velocity fluctuations relative to the SPAM-smoothed field velocities, and to determine the intrinsic viscosity as a function of density in a set of separate shear-flow simulations [12].

Acknowledgements

We gratefully acknowledge the financial support from the *Fonds zur Förderung der wissenschaftlichen Forschung* under grant P11428, and the generous allocation of computer resources by the Computer Center of the University of Vienna. A part of this work was performed at the Lawrence Livermore National Laboratory under the auspices of the United States Department of Energy through University of California Contract W-7405-Eng-48.

References

- [1] H.E. Trease, M.J. Fritts, W.P. Crowley (Eds.), *Advances in the Free-Lagrange Method*, Lecture Notes in Physics, vol. 395, Springer, Berlin, 1991.
- [2] J.J. Monaghan, *Comp. Phys. Rep.* 3 (1985) 71.
- [3] J.F. Wendt (Ed.), *Computational Fluid Dynamics*, Springer, Berlin, 1992.
- [4] L.B. Lucy, *Astron. J.* 82 (1997) 1013.
- [5] R.A. Gingold, J.J. Monaghan, *MNRAS* 181 (1977) 375.
- [6] *Comp. Phys. Comm.* 48 (1988) 97.
- [7] J.J. Monaghan, *Ann. Rev. Astron. Astrophys.* 30 (1992) 543.
- [8] M. Steinmetz, E. Müller, *Astron. Astrophys.* 268 (1993) 391.
- [9] H. Riffert, H. Herold, O. Fiebbe, H. Ruder, *Comp. Phys. Comm.* 89 (1995) 1.
- [10] R.F. Stellingwerf, *Lecture Notes in Physics* 395 (1991) 239.
- [11] H. Takeda, S.M. Miyama, M. Sekiya, *Progr. Theor. Phys. Japan* 92 (1994) 939.
- [12] H.A. Posch, W.G. Hoover, O. Kum, *Phys. Rev. E* 52 (1995) 1711.
- [13] O. Kum, W.G. Hoover, H.A. Posch, *Phys. Rev. E* 52 (1995) 4899.
- [14] W.G. Hoover, S. Hess, *Physica A*, 231 (1996) 425.
- [15] O. Kum, W.G. Hoover, *J. Stat. Phys.* 76 (1994) 10075.
- [16] W.G. Hoover, H.A. Posch, *Phys. Rev. E*, 54 (1996) 5142.
- [17] L.D. Meshalkin, Ya.G. Sinai, *J. Appl. Math.* 25 (1961) 1700.
- [18] J.S.A. Green, *J. Fluid Mech.* 62 (1974) 273.
- [19] G.I. Sivashinsky, *Physica D* 17 (1985) 243.